

Influence of defects on transport in quasi-one-dimensional arrays of chains of metal atoms on silicon

Hiroyuki Okino, Iwao Matsuda, Rei Hobara, and Shuji Hasegawa*

Department of Physics, School of Science, University of Tokyo, 7-3-1 Hongo, Bunkyo-ku, Tokyo 113-0033, Japan

Younghoon Kim and Geunseop Lee[†]

Inha University, Incheon 402-751, Korea

(Received 17 June 2007; published 15 November 2007)

Conductivities of quasi-one-dimensional metallic atomic-chain (AC) arrays of Si(553)-Au and Si(111)4 × 1-In surfaces were measured by a rotational square micro-four-point probe method. This method provided the conductivity along the ACs (σ_{\parallel}) and that across them (σ_{\perp}) separately. While the measured σ_{\parallel} of the 4 × 1-In was nearly half of σ_{\parallel} expected from the surface-state band structure, the σ_{\parallel} of the Si(553)-Au was more than 1 order of magnitude smaller than the value expected from the bands. This was attributed to dense intrinsic point defects on the Si(553)-Au. We demonstrated that point defects on the ACs really decreased the σ_{\parallel} value by intentionally introducing defects on the 4 × 1-In with oxygen adsorption.

DOI: [10.1103/PhysRevB.76.195418](https://doi.org/10.1103/PhysRevB.76.195418)

PACS number(s): 73.25.+i, 68.37.Ef, 81.07.Vb

I. INTRODUCTION

The role of defects, in general, can be constructive and destructive in device applications. The defects create carriers in semiconductors by doping, whereas they become scattering centers or induce random potential. The effects of defects are relatively enhanced and become significant when the device size shrinks in reduced dimension even at room temperature (RT). Indeed, surface defects have a large influence on the carrier mobility in 5-nm-diameter Si nanowires (NWs).¹ A theoretical calculation showed that transport properties of the 1.5-nm-diameter Si NWs were very sensitive to disorder in the surface, whereas bulk disorder has almost no influence.² Thus, in the extreme limit, i.e., in a layer of 1 ML (monolayer) thickness, the defects are expected to play a significant role in transport.

So far, anisotropic conductivity of metallic atomic-chain (AC) arrays of 1 ML thickness has been measured only for Si(111)4 × 1-In (4 × 1-In in short hereafter)³ and Si(557)-Au surfaces.⁴ The 4 × 1-In is nearly defect-free, whereas the Si(557)-Au has a much higher density of point defects, as shown in scanning tunneling microscope (STM) images of Figs. 1(a) and 1(b), respectively. The conductivity in these quasi-one-dimensional (quasi-1D) metallic systems is expressed by different values in two orthogonal directions: a highly conductive direction (parallel to the ACs, σ_{\parallel}) and a poorly conductive direction (perpendicular to the ACs in the plane, σ_{\perp}). The reported anisotropy ($\sigma_{\parallel}/\sigma_{\perp}$) was about 60 for the 4 × 1-In,³ while only 2.7 for the Si(557)-Au.⁴ Although the Fermi surface of Si(557)-Au is more one-dimensional-like (1D-like) than that of the 4 × 1-In,⁵⁻⁸ the anisotropy of the Si(557)-Au is much smaller. This suggests that the point defects reduce the σ_{\parallel} value, not the σ_{\perp} .

To confirm the role of defects, we measured anisotropic conductivity of defective quasi-1D AC arrays formed on Si substrates, Si(553)-Au, and oxygen-exposed 4 × 1-In surfaces. Figures 1(c) and 1(d) show their STM images. The thickness of the ACs is 1 ML for both, and the width is 1.5 nm for the Si(553)-Au and 1.3 nm for the 4 × 1-In. The ACs of the Si(553)-Au are separated from each other by

monatomic steps (0.31 nm height), whereas the ACs of 4 × 1-In are basically on the same terraces. The Si(553)-Au is metallic at RT with quasi-1D Fermi surfaces.^{5,9} In spite of the presence of a lot of point defects as shown in Fig. 1(d), clear Fermi surfaces are visible in photoemission spectroscopy. Although the defects look like vacancies in the STM image, the identity and the actual size of the defects are unknown. However, it is certain that the metallic ACs are cut into metallic segments by these defects.^{10,11} On the other hand, the pristine 4 × 1-In has few defects, as shown in Fig. 1(a), which also shows quasi-1D Fermi surfaces with slightly larger interchain interaction.⁷ We introduced intentionally extrinsic defects on the 4 × 1-In by exposing it to oxygen to create point defects, as shown in Fig. 1(c),¹² where 10 L oxygen gas was dosed (1 L = 1 × 10⁻⁶ Torr s).

From the conductivity measurement, we determined both σ_{\parallel} and σ_{\perp} separately and compared the results with the conductivities estimated by using Boltzmann equation combined with the surface-state band dispersions reported previously.^{3,5} The measured σ_{\parallel} of the pristine 4 × 1-In was nearly half of the estimated conductivity, whereas that of the Si(553)-Au was much smaller than the value estimated from the bands. This was attributed to the presence of dense

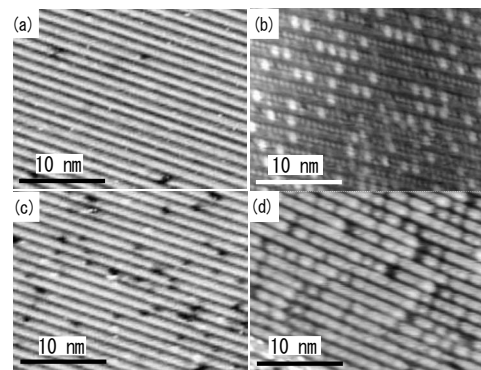


FIG. 1. STM images of the (a) pristine 4 × 1-In, (b) Si(557)-Au, (c) 10 L O₂-exposed 4 × 1-In, and (d) Si(553)-Au. The tip bias was (a) 1.4 V, (b) -2.0 V, (c) 1.4 V, and (d) 2.0 V.

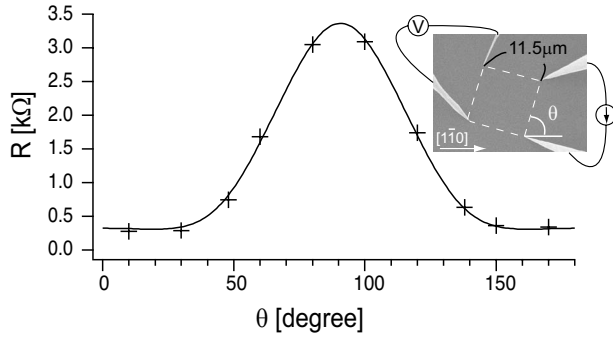


FIG. 2. Dependence of the measured resistance of the Si(111) 4×1 -In on the rotation angle of the square. The solid line is a fit to a theoretical function derived in Ref. 3, in which the fitting parameters are σ_{\parallel} , σ_{\perp} , and θ . The inset is an SEM image of the four tips, in which the square is highlighted by white broken lines.

atomic-scale point defects on the ACs of the Si(553)-Au. The effect of point defects on quasi-1D ACs was verified by observing a dramatic decrease in σ_{\parallel} , not in σ_{\perp} , with introducing defects by oxygen adsorption on the 4×1 -In.

II. EXPERIMENT

The Si(553)-Au was formed by depositing 0.24 ML Au onto a heated Si substrate held at 650 °C, followed by annealing at 850 °C. The substrate was a P-doped *n*-type vicinal wafer having a resistivity of 1–10 Ω cm at RT, which was inclined to the $[11\bar{2}]$ direction by 12.5° from (111).^{9,13} The 4×1 -In surface was formed by depositing 1 ML In onto a heated Si substrate held at 450 °C. The substrate was a P-doped *n*-type vicinal Si(111) having a resistivity of 1–10 Ω cm at RT. The surface normal direction was inclined to the $[\bar{1}1\bar{2}]$ direction by 1.8° to make the single-domain structure because the ACs grew along the step direction.⁷ Oxygen gas was dosed at RT by backfilling the chambers.

Anisotropy in the conductivity was measured *in situ* by a rotational square micro-four-point probe (M4PP) method by using a four-tip STM.^{3,14} Four tungsten tips directly touched the sample surface during the measurements. The tips were placed in a square on the sample surface under observation by a scanning electron microscope (SEM). A side of the square was 10–20 μ m. In the rotational square M4PP method,³ the square is rotated with respect to the sample surface step by step, and the conductivity is measured at different angles θ of rotation, as shown in the inset in Fig. 2. The resistance data are fitted to a theoretical function with fitting parameters σ_{\parallel} , σ_{\perp} , and θ .³ Then, we can obtain σ_{\parallel} and σ_{\perp} separately and also the anisotropy $\sigma_{\parallel}/\sigma_{\perp}$.

Since the ACs are not freestanding, but on Si substrates, the measured conductivity contains contributions not only from the atomic chains (σ_{AC}) but also from the surface space-charge layer (σ_{SC}) as well as bulk substrate (σ_B). We have confirmed, however, that the measured conductivity was expressed as a sum of σ_{AC} and σ_{SC} only.^{3,15} The anisotropy in conductivity comes only from σ_{AC} because the surface space-charge layer beneath the surface is isotropic.

III. RESULTS AND DISCUSSION

Figure 2 shows the resistance of the 4×1 -In as a function of rotation angle θ , with a theoretical fit to the data points. The conductivity of the pristine 4×1 -In was $\sigma_{\parallel} \sim 310 \mu\text{S}/\square$ and $\sigma_{\perp} \sim 18 \mu\text{S}/\square$, and then the anisotropy ($\sigma_{\parallel}/\sigma_{\perp}$) was 17. The previously reported anisotropy of the 4×1 -In was about 60,³ which indicates that our 4×1 -In sample might be more defective. The conductivity of the Si(553)-Au was $\sigma_{\parallel} \sim 82 \mu\text{S}/\square$ and $\sigma_{\perp} \sim 30 \mu\text{S}/\square$, and then the anisotropy was 2.7. The anisotropy of the 4×1 -In is much higher than that of the Si(553)-Au, although the Si(553)-Au is expected to show a larger anisotropy by considering the band structures as shown below.

The σ_{AC} can be estimated from the known surface-state band structures using the Boltzmann equation in two dimensions,¹⁶

$$\sigma_{ij} = \frac{1}{2\pi^2} \frac{e^2}{\hbar} \int \tau_{ij}(\mathbf{k}) \frac{v_i(\mathbf{k})v_j(\mathbf{k})dk_F}{|\mathbf{v}(\mathbf{k})|}, \quad (1)$$

where τ_{ij} is a tensorial relaxation time, and the integral is done on the Fermi surface. Here, we show the calculation about the Si(553)-Au for an example. The group velocity [$\mathbf{v}(\mathbf{k}) = \nabla_{\mathbf{k}} E(\mathbf{k})/\hbar$] was calculated using the band dispersion reported in Ref. 5. The relaxation time is, in principle, anisotropic ($\tau_{\parallel} \neq \tau_{\perp}$). In addition, the relaxation time is k dependent, since the relaxation depends on k -dependent scattering direction and scattering probability. However, for simplicity, we assume an isotropic and k -independent relaxation time by taking the average values, $\langle \tau_{\parallel} \rangle$ and $\langle \tau_{\perp} \rangle$. Though these assumption and simplification cause some errors, the order of magnitude of σ_{AC} could be estimated. The relaxation time can be estimated experimentally from peak broadening in photoemission spectra;¹⁷ the momentum width of a photoemission peak is equal to $1/\lambda$, where λ is a mean free path of carriers. From the reported photoemission spectra at ~ 200 K in Ref. 9, we estimated the carrier mean free path to be 3.0 nm, and then the relaxation time ($\tau = \lambda/v_F$) to be 3.8×10^{-15} s. We used this value for τ in the calculation. Because the Si(553)-Au has three surface-state bands crossing E_F , we have to add their contributions. However, the character of the three bands is still controversial.^{9,18,19} Thus, we assume here that one band is a spin-degenerate metallic band and the other two are spin-split metallic bands.¹⁹ As a result, the estimated σ_{AC} in the parallel direction was approximately 600 $\mu\text{S}/\square$ and approximately 6.4 $\mu\text{S}/\square$ in the perpendicular direction. The calculation used the relaxation time at ~ 200 K, which was lower than our measurement temperature (RT), but the order of magnitude might be similar to that at RT. For the 4×1 -In, Kanagawa *et al.* calculated σ_{AC} in the same way.³ By combining the relaxation time obtained from the photoemission, the conductivities in parallel and perpendicular directions are estimated in the same way.

In order to evaluate the total conductivity, we have to add isotropic σ_{SC} to the above-calculated σ_{AC} . We have estimated σ_{SC} of the Si(553)-Au and the 4×1 -In by using Poisson's equation with the known band bending, giving $\sigma_{SC} \sim 15 \mu\text{S}/\square$ for both surfaces as in the previous studies.^{3,15} Thus, the sums of σ_{AC} and σ_{SC} in each direction should be

TABLE I. The measured and calculated conductivities of the Si(557)-Au, Si(553)-Au, and 4×1 -In, together with the average length ($\langle L \rangle$) of the defect-free segments in ACs.

	Si(557)-Au		Si(553)-Au		4×1 -In	
	Meas. ^a	Calc. ^b	Meas.	Calc. ^c	Meas.	Calc. ^d
σ_{\parallel} ($\mu\text{S}/\square$)	9.3	200	82	620	310	680
σ_{\perp} ($\mu\text{S}/\square$)	3.5	0.36	30	21	18	50
Anisotropy ($\sigma_{\parallel}/\sigma_{\perp}$)	2.7	560	2.7	29	17	14
$\langle L \rangle$ [nm]	5		10		100	

^aReference 4.

^bThe relaxation time was estimated from the width of a momentum distribution curve reported in Ref. 6, which was 3.1×10^{-15} s at 100 K.

^cThis column shows the values at ~ 200 K.

^dThe calculation of σ_{AC} used the relaxation time of 4.9×10^{-15} s estimated from photoemission.

compared with the measured conductivity. The results obtained for the Si(553)-Au and the 4×1 -In are listed in Table I, together with the values of the Si(557)-Au reported in Ref. 4 for reference. At a glance, while the 4×1 -In shows a slight decrease of the measured σ_{\parallel} value from the calculated one, the Si(557)-Au and Si(553)-Au show quite a large discrepancy between the two values in σ_{\parallel} . The measured values are much smaller than the calculated ones. The anisotropy shows a similar tendency.

The cause of the reduction in σ_{\parallel} might be attributed to the point defects on the ACs: the point defects interrupt the AC, which decreases σ_{\parallel} in Si(553)-Au and Si(557)-Au. The point defects induce a local $\times 2$ modulation along the ACs.^{12,20,21} This induced potential strongly scatters the carriers because the wave number of the potential modulation corresponds to $2k_F$ so that the Bragg reflection takes place (where k_F is the Fermi wave number). Generally speaking, scattering by point defects broadens photoemission spectroscopy (PES) spectra,⁵ and thus the estimated $\langle \tau \rangle$ from spectrum broadening should include the influence of the defects. However, the large difference between the measured and the calculated anisotropy for the Si(553)-Au and the Si(557)-Au indicates that the influence of the defects on transport is larger than that on electronic states. This may be seen by comparing the mean free path of carriers λ determined by PES and the average length of the AC segments. Average lengths of ACs ($\langle L \rangle$) segmented by point defects are estimated from STM images and also listed in Table I. The Si(553)-Au and the Si(557)-Au have $\langle L \rangle$ values comparable to the λ of carriers flowing along the ACs, causing severe scattering in the transport and thus large reduction of σ_{\parallel} . In contrast, the 4×1 -In has much longer chain segments (large $\langle L \rangle$), explaining the same magnitude of conductivity between the measured and calculated ones.

We have tested the above interpretation about the influence of point defects on the decrease of σ_{\parallel} by intentionally introducing extrinsic defects on the 4×1 -In. The 4×1 -In was exposed to O_2 gas at RT, which created point defects, as shown in Fig. 1(c). The defect density increased almost linearly with the dose, as shown in Fig. 3(a). Figure 3(b) shows the change of σ_{\parallel} and σ_{\perp} with the O_2 dosage, measured by the M4PP method. The σ_{\parallel} decreased drastically, whereas σ_{\perp} remained unchanged, which led to the reduction of the an-

isotropy with the O_2 adsorption. The $\langle L \rangle$ of the O_2 -adsorbed 4×1 -In for 10 L was reduced to 7 nm, which was comparable to the estimated mean free path of several nanometers along the ACs.

In addition, the results also show that the contribution of SC layer in σ is isotropic despite the monatomic step arrays on a vicinal Si substrate. We used a vicinal Si substrate for making the single-domain 4×1 -In, which contains one step (0.31 nm height) per 10-nm-wide terrace on average. The measured conductivity in Fig. 3(b) is a sum of the defective atomic-chain conductivities σ_{AC} and σ_{SC} . The σ_{\parallel} decreases with O_2 dosage and becomes equal to σ_{\perp} at 15 L: the sample is isotropic. The absence of the anisotropy in the space-

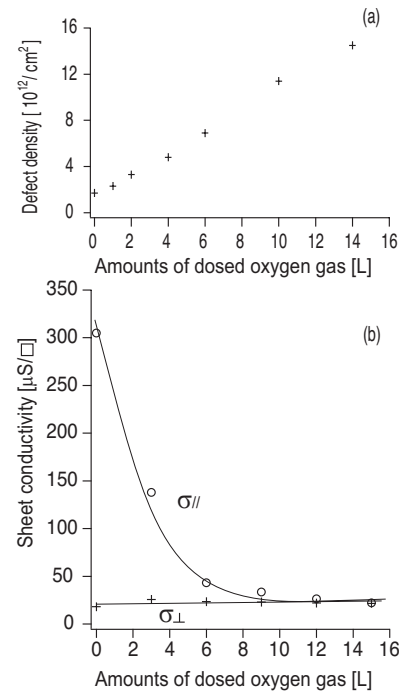


FIG. 3. (a) The density of defects on the 4×1 -In created by dosing O_2 gas, estimated from STM images. (b) Conductivity parallel (circle) and perpendicular (cross) to the ACs of the 4×1 -In as a function of the amount of dosed O_2 gas. Solid lines are a guide for the eye.

charge layer even in the presence of the monatomic steps may be explained as follows. At RT, the carrier mean free path in the Si substrate at RT is much shorter than the thickness of the space-charge layer (several hundreds of nanometers), and the carrier wavelength in Si is much larger than the step height (0.31 nm). Thus, classical and quantum size effects were absent in the space-charge layer.

We have to note that the monatomic steps usually cause resistance in transport through the outermost layer of 1 ML thickness as reported in a surface free-electron-gas system.²² For σ_{AC} of the Si(553)-Au, however, in which each AC is separated by monatomic steps, it is not necessary to think of the steps as additional scatterers. This is because the steps are periodic along the step-normal direction, and thus the effect of the steps is included in the band structure. For the calculation of the anisotropy of σ_{AC} , we have only to consider the band structure as mentioned before using the Boltzmann equation.

IV. CONCLUSIONS

In summary, σ_{\parallel} and σ_{\perp} of quasi-1D AC arrays of the Si(553)-Au and the 4×1 -In were measured and compared

with the results of Si(557)-Au. The σ_{\parallel} 's of the Si(553)-Au and Si(557)-Au were much smaller than the values expected from the surface-state band structure, whereas σ_{\parallel} of the 4×1 -In was nearly half of the value calculated from the bands. The difference was related to the density of point defects on the ACs: the Si(553)-Au and Si(557)-Au have much higher densities of defects than the 4×1 -In. Because the ACs are 1 ML thick, the point defects effectively block the conduction carriers along the ACs. We have demonstrated that point defects are critical in one dimension by introducing extrinsic defects on the 4×1 -In with oxygen adsorption, which showed a drastic decrease of σ_{\parallel} .

ACKNOWLEDGMENTS

This work has been supported by Grants-In-Aid, Japan-Korea Joint Research Project, and A3 Foresight Program from the Japanese Society for the Promotion of Science. G.L. is supported by the Joint Research Program funded by the Korea Science and Engineering Foundation (F01-2005-000-10279-0) and by the Korea Research Foundation Grant funded by the Korean Government (MOEHRD) (R02-2004-000-10262-0).

*Corresponding author; shuji@surface.phys.s.u-tokyo.ac.jp

†Corresponding author; glee@inha.ac.kr

¹Y. Cui, D. Wang, W. U. Wang, and C. M. Lieber, *Nano Lett.* **3**, 149 (2003).

²T. Markussen, R. Rurali, M. Brandbyge, and A.-P. Jauho, *Phys. Rev. B* **74**, 245313 (2006).

³T. Kanagawa, R. Hobara, I. Matsuda, T. Tanikawa, A. Natori, and S. Hasegawa, *Phys. Rev. Lett.* **91**, 036805 (2003).

⁴H. Okino, R. Hobara, I. Matsuda, T. Kanagawa, S. Hasegawa, J. Okabayashi, S. Toyoda, M. Oshima, and K. Ono, *Phys. Rev. B* **70**, 113404 (2004).

⁵J. N. Crain, J. L. McChesney, F. Zheng, M. C. Gallagher, P. C. Snijders, M. Bissen, C. Gundelach, S. C. Erwin, and F. J. Himpsel, *Phys. Rev. B* **69**, 125401 (2004).

⁶R. Losio, K. N. Altmann, A. Kirakosian, J. L. Lin, D. Y. Petrovykh, and F. J. Himpsel, *Phys. Rev. Lett.* **86**, 4632 (2001).

⁷H. W. Yeom, S. Takeda, E. Rotenberg, I. Matsuda, K. Horikoshi, J. Schaefer, C. M. Lee, S. D. Kevan, T. Ohta, T. Nagao, and S. Hasegawa, *Phys. Rev. Lett.* **82**, 4898 (1999).

⁸J. R. Ahn, J. H. Byun, H. Koh, E. Rotenberg, S. D. Kevan, and H. W. Yeom, *Phys. Rev. Lett.* **93**, 106401 (2004).

⁹J. N. Crain, A. Kirakosian, K. N. Altmann, C. Bromberger, S. C. Erwin, J. L. McChesney, J. L. Lin, and F. J. Himpsel, *Phys. Rev. Lett.* **90**, 176805 (2003).

¹⁰J. N. Crain, M. D. Stiles, J. A. Stroscio, and D. T. Pierce, *Phys.*

Rev. Lett. **96**, 156801 (2006).

¹¹J. N. Crain and D. T. Pierce, *Science* **307**, 703 (2005).

¹²G. Lee, S.-Y. Yu, H. Kim, and J.-Y. Koo, *Phys. Rev. B* **70**, 121304(R) (2004).

¹³H. Okino, I. Matsuda, T. Tanikawa, and S. Hasegawa, *e-J. Surf. Sci. Nanotechnol.* **1**, 84 (2003).

¹⁴I. Shiraki, F. Tanabe, R. Hobara, T. Nagao, and S. Hasegawa, *Surf. Sci.* **493**, 633 (2001); S. Hasegawa, I. Shiraki, F. Tanabe, and R. Hobara, *Curr. Appl. Phys.* **2**, 465 (2002).

¹⁵H. Okino, I. Matsuda, S. Yamazaki, R. Hobara, and S. Hasegawa, *Phys. Rev. B* **76**, 035424 (2007).

¹⁶T. Hamaguchi and K. Taniguchi, *Physics of Semiconductor Device* (Asakura, Tokyo, 1990), in Japanese.

¹⁷Y.-D. Chuang, A. D. Gromko, D. S. Dessau, T. Kimura, and Y. Tokura, *Science* **292**, 1509 (2001).

¹⁸J. R. Ahn, P. G. Kang, K. D. Ryang, and H. W. Yeom, *Phys. Rev. Lett.* **95**, 196402 (2005).

¹⁹I. Barke, F. Zheng, T. K. Rugheimer, and F. J. Himpsel, *Phys. Rev. Lett.* **97**, 226405 (2006).

²⁰H. W. Yeom, J. R. Ahn, H. S. Yoon, I. W. Lyo, H. Jeong, and S. Jeong, *Phys. Rev. B* **72**, 035323 (2005).

²¹P. C. Snijders, S. Rogge, and H. H. Weitering, *Phys. Rev. Lett.* **96**, 076801 (2006).

²²I. Matsuda, M. Ueno, T. Hirahara, R. Hobara, H. Morikawa, C. Liu, and S. Hasegawa, *Phys. Rev. Lett.* **93**, 236801 (2004).